JOURNAL GEOLOGICAL SOCIETY OF INDIA
Vol.95, January 2020, pp.17-24

The "Lower Kaimur Porcellanite" (Vindhyan Supergroup) is of Sedimentary Origin and not Tuff

Adrita Choudhuri[1], Juergen Schieber[2], Subir Sarkar[3], Marion E. Bickford[4], and Abhijit Basu[2*]

[1]Department of Earth Sciences, Indian Institute of Science Education and Research, Mohanpur Campus, Kolkata - 741 246, India
[2] Department of Earth and Atmospheric Sciences, Indiana University, Bloomington, IN 47405, U.S.A.
[3]Department of Geological Sciences, Jadavpur University, Kolkata - 700 032, India
[4]Department of Earth Sciences, Heroy Geology Laboratory, Syracuse University, Syracuse, New York 13244-1070, USA
***E-mail:** *basu@indiana.edu*

ABSTRACT

The 'Lower Kaimur Porcellanite' from the Proterozoic Vindhyan Supergroup (~1700-900? Ma) is not only a chrono-stratigraphic marker but also an indicator of the tectonic setting of the basin. A few other silicified shaly units (porcellanites) from the upper strata have been thought to be tuff. New petrographic (optical microscopic; SEM-BSE), chemical, and U-Pb zircon geochronological studies of the lowermost of these suspected tuff units, however, do not support an igneous origin for these beds. The rocks do not contain phenocrysts or glass shards, but contain remains of mineralized microbial spheres, mudclasts, and other detrital grains that include one datable zircon grain (~1715 Ma). Their chemical compositions are not diagnostic of tuff. Despite this result, investigations of other porcellanites from Upper Vindhyan strata is recommended, because they have the potential of identifying crucially important tuff beds.

INTRODUCTION

Background and Purpose

During the "rather 'boring'" billion years of Earth history (1.85 – 0.85 Ga; Holland, 2006), large quantities of sediments were deposited in different basins in Peninsular India. The basins were floored by continental crust and developed in and around several cratons of the old supercontinent Ur (Rogers, 1996). Most of these sediments survived as sub-horizontally bedded or mildly deformed and un-metamorphosed rock strata, commonly called *Purana* strata (Radhakrishna, 1987).

Fine grained and at places very thinly bedded silicified strata occurring in *Purana* basins were mapped as porcellanites, of which the Porcellanite Formation in the Vindhyan basin (Auden, 1933; Ghosh, 1971; Chakraborty, 2006) is the best known. Felsic volcanism, at about 1640-1630 Ma (Ray et al., 2002; Rasmussen et al., 2002; Mishra et al., 2018), ~1500-1400 Ma (Das et al., 2009; Bickford et al., 2011a; Das et al., 2015), and ~1000 Ma (Patranabis-Deb et al, 2007; Bickford et al., 2011b; Mukherjee et al., 2012), deposited ash and rhyolitic flow-breccia in several *Purana* basins. Interestingly, all of these volcanic deposits in the *Purana* basins have been silicified, to various extent during diagenesis, silicified tuff being the most abundant. Many felsic volcanic units including ash flows, have been discovered in *Purana* basins in the last twenty years or so including, for example, Singhora Tuff (Chakraborti, 1997), Sukhdah tuff (Denduluri et al., 2006), and Dhamda tuff (Bickford et al., 2011b) in the Chhattisgarh basin; the Katingapani tuff in the Khariar basin (Das et al., 2009); Birsaguda tuff in the Indravati basin (Mukherjee et al., 2012); and "Pipalchapar" tuff in the Ampani basin (Das et al., 2015). However, many porcellanites may be silicified shale beds and not tuff. For example, a promising lead of a silicified bed in the Owk shale in the Cuddapah basin (Saha and Tripathy, 2012), unfortunately, proved to be a silicified shale bed (Bickford et al., 2013).

Chakraborty et al. (1996) identified several silicified mudstone beds containing evidence of felsic volcanism in the Kaimur and Rewa Groups in the Vindhyan basin (aka Vindhyanchal basin; Kale 2016). Petrographic (optical microscopic; SEM-BSE), chemical, and U-Pb zircon geochronological studies of the lowermost of these suspected tuff beds, which belongs to the Kaimur Group were conducted. The findings however, do not support an igneous (~volcanic) origin for these beds.

GEOLOGICAL SETTING

General

The Vindhyan Supergroup consists of four Groups – Semri, Kaimur, Rewa, and Bhander (Table 1; Ramakrishnan and Vaidyanadhan, 2010). A basin-wide unconformity, putatively representing a hiatus of about 400 m.y. (Tripathy and Singh, 2015) and changes in depositional facies, occurs above the Semri Group (Bose et al., 2001; Sarkar et al., 2002a,b, 2004, 2005). A bimodal, medium to coarse-grained, silica-cemented quartz arenite, called Sasaram Sandstone in the east and Lower Kaimur Sandstone/Quartzite in the rest of the basin, occurs at the base of the Kaimur Group. It rests on the carbonates and argillaceous rocks of the Semri Group with a sharp disconformity (Gupta et al., 2003; Sen et al., 2014; Quasim and Ahmad, 2015; Quasim et al., 2017). A 12 m thick "shale member", with several silicified beds called porcellanite, (Chakraborty et al., 1996) interbedded with thin sandstone and shale beds, lies above the prominent sandstone of the lower Kaimur Formation (aka Sasaram sandstone). Mandal et al. (2019) consider this porcellanite-bearing unit as part of Sasaram sandstone. These porcellanite beds are the focus of the present investigation.

Occurrence of the "Lower Kaimur Porcellanite" (LKP)

LKP occurs continuously for at least 100 km and thins from about 10 m to about 3 m from Badanpur (24°10'28.68"N, 80°51'19"E) near Maihar in the west, to Baghwar (24°19'51.04"N, 81°24'30.72"E) near Rampur in the east (Fig.1). This unit consistently occurs above the Lower Kaimur Sandstone that developed within a tide-dominated shelf with rare stormy interventions (Chakraborty and Bose, 1992). LKP is principally composed of shale, with sand-silt alternations. The color

0016-7622/2020-95-1-17/$ 1.00 © GEOL. SOC. INDIA | DOI: 10.1007/s12594-020-1382-7

Table 1. Relevant section of the stratigraphy of the Vindhyan Supergroup in the study area

Vindhyan Supergroup	Bhander Group	Upper Bhander Sandstone Sirbu Shale Lower Bhander Sandstone Bhander Limestone Ganurgarh Shale
	Rewa Group	Rewa Sandstone Rewa Shale
	Kaimur Group	Dhandraul Quartzite/Mangeswar Formation (= Scarp Sandstone) Lower Kaimur Porcellanite Lower Kaimur (Sasaram) Sandstone
	Semri Group	Rohtas Fm Kheinjua Fm Porcellanite Fm Kajrahat Fm Deoland Fm
Basement		

of the shale varies, both vertically as well as laterally, from grey to dark grey, and is even black at places. The sand/silt stringers present within the shale are sheet-like and laterally continuous; some of these sand beds have an undulatory basal contact with the shale and bear sole features that indicate deposition within a shelf where sand could ingress only during storm/high energy periods. Thinly bedded porcellanite units (individual thickness varying from 15 cm to 35 cm) occur within LKP at different stratigraphic levels (Chakraborty PP., 2006). Conchoidal joint planes are observed within these porcellanite beds. In the outcrop extent between Maihar and Rampur, Markundi Sandstone and Bijaigarh Shale are absent. Thus, in this locality, LKP is overlain by the Scarp Sandstone /Mangeswar Formation, deposited in a fluvio-aeolian environment (Bhattacharya and Morad, 1993). It is apparent that the transition from a shelf to fluvial-aeolian environment marks a major fall in sea level (Chakraborty et al., 1996).

SAMPLES AND ANALYSES

13 samples were collected from LKP at three locations along the studied outcrop extent (Fig. 2). At outcrop scale, the appearance of these porcellanite beds (Fig. 3a, b) is not different from silicified ash beds elsewhere. Polished extra-thin and standard thin sections of the samples were used for petrographic study, including transmitted and reflected light optical microscopy, back scattered electron (BSE) SEM images, and energy dispersive spectra on spots for phase identification. Chemical compositions of the samples were obtained from Activation Lab (Ancaster, Canada), using their high precision 4E-Research and 4E-ICPMS packages. The samples are very fine-grained; thus, despite repeated attempts, including those by GeoSep Services (Moscow, ID, USA), only two grains of reliably analyzable zircon could be separated, one of which was barely large enough to provide separate core and rim ages. The analyses were conducted in the LA-MC-ICPMS facilities at the University of Florida (Bickford et al., 2014).

RESULTS AND INFERENCES

Petrography: Optical microscopic observations show that the samples are fine-grained mudstones with a few coarse, silt-size, irregularly-shaped quartz grains; these lack embayment, triangular shapes, and sector or oscillatory zoning. They are not phenocrysts. Feldspars are not readily identifiable. A few larger elongate particles are opaque, and may be carbonaceous streaks (Fig. 4a). Dusty and somewhat equidimensional grains, opaque in transmitted light and yellowish in reflected light, are pyrite (confirmed by SEM-EDS). Non-opaque elongate grains are muscovite (confirmed by SEM-EDS). In one sample (P8), there are spots of deferruginized clay (Fig. 4b). No phenocrysts are found in any of the thin sections of the 13 samples.

SEM-BSE-EDS observations confirm further the absence of

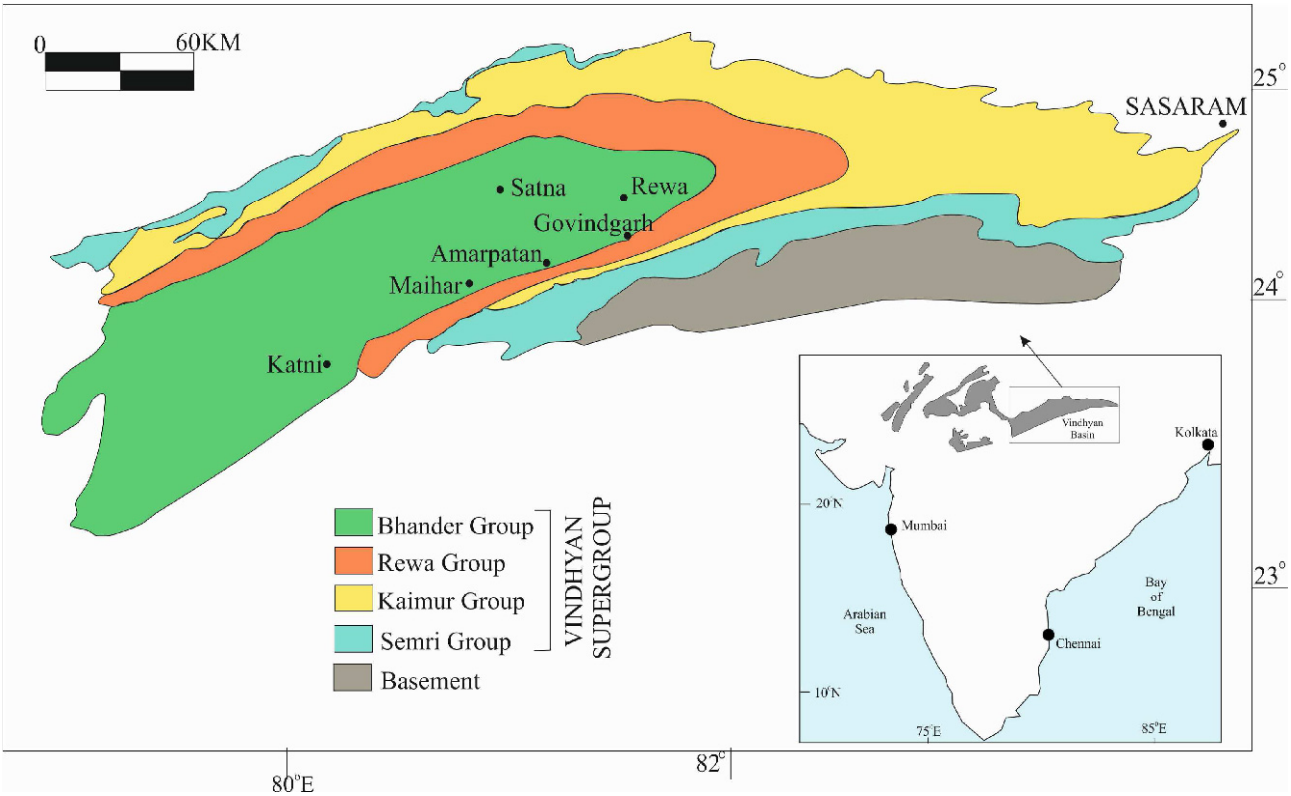

Fig.1. Generalized geological map of the Vindhyan Supergroup showing major cities near sample sites.

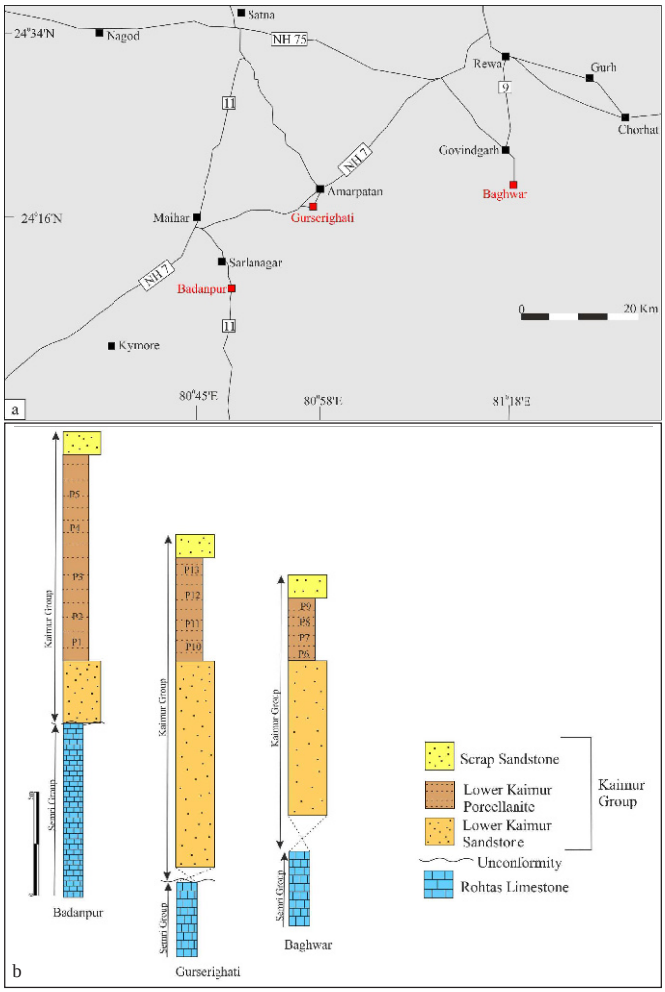

Fig.2. Details of **(a)** geographic locations (in red) and **(b)** stratigraphic positions of the samples.

phenocrysts. The matrix is silicified, and nearly all discernible grains are quartz grains and clays <20 μm in size. Many of the larger quartz grains have serrated edges, possibly a result of dissolution during diagenesis. Muscovite is common and at places is altered to kaolinite (Fig. 5A,B). The shapes of surface cavities in the thin sections suggest that pyrite was plucked out during thin section preparation or dissolved during outcrop weathering (Fig. 6). Elongate dark patches are carbonaceous, suggesting that they are compressed fragments of microbial mats (Schieber, 1989; Schieber et al., 2007; Fig. 7). Scattered grains of aggregated silt size particles were also observed; they are possibly mudstone lithics recycled from older strata (Schieber, 2016; Fig. 7). Cross-sections of apatite-mineralized microbial spheres occur in a few mudclasts and as isolated particles (Figs. 5 and 7). These spheres are identical to the microbial spheres observed in the Bijaigarh Shale in the middle of the Kaimur Group (see fig. 7-G,H in Schieber et al., 2007).

Geochemistry: The chemical composition of LKP (Table 2) does not indicate a volcanic origin unless most of the original characteristics have been obliterated by diagenesis. The bed is highly silicified; on a LOI-free basis, SiO_2 is >90%, Al_2O_3 is ~ 6%, and, Na_2O (0.07%) and K_2O (1.36%) are very low. In the porcellanites (silicified ash/tuff) of the Semri Group, Na_2O and K_2O are much higher (1.74% and 3.16% respectively; Mishra et al., 2017; Bickford et al., 2017). TiO_2 normalized values of Na_2O and K_2O (0.5 and 10.1 respectively) in LKP are also much lower than those in the Semri porcellanite (11.3 and 20.5 respectively). Trace element distributions are generally equivocal. The moderate negative Eu anomaly (0.6) is not diagnostic. A minor negative Ce anomaly (0.8) may be a product of diagenesis under reducing conditions (e.g., Shields and Stille, 2001; Basu et al., 2016) or due to mixing (Bellot et al., 2018); it is not diagnostic. The strong correlations between Rb and K_2O (r = 0.98) and between Th and Sc (r = 0.88) may suggest that only two separate single (mineral?) phases primarily host these elements, a condition not generally expected in volcanic ash.

Geochronology: The very fine-grained nature of this porcellanite bed stymied the efforts to separate zircons and obtain meaningful U-Pb ages. Only ten zircon grains were separted, knowing that not all (e.g., Fig. 8) were large enough and inclusion-free for reliable U-Pb analysis. The core and the rim of only one grain (Fig. 9) provided 1725 ± 18 Ma and 1706 ± 18 Ma as reliable ages. These ages are comparable to the ages from the basement rock units of the Vindhyan Supergroup (e.g., 1753 ± 9 Ma for the Jhirgadandi pluton; Bora et al., 2013) and suggest that this zircon grain is detrital. A coeval magmatic zircon in a volcanic ash bed in the Kaimur would likely have been <<1630 Ma (Semri porcellanite; Mishra et al., 2018) and possibly close to 1200 Ma (Kaimur - black shale; Tripathy and Singh, 2015) in age.

Petrographic, geochemical, and geochronological properties indicate that porcellanite beds in LKP are not tuff and are very likely silicified mudstones.

DISCUSSION

"Porcellanite" (Calcera, 1847; p. 5) is a non-technical term to informally name rocks with the "… general appearance of unglazed

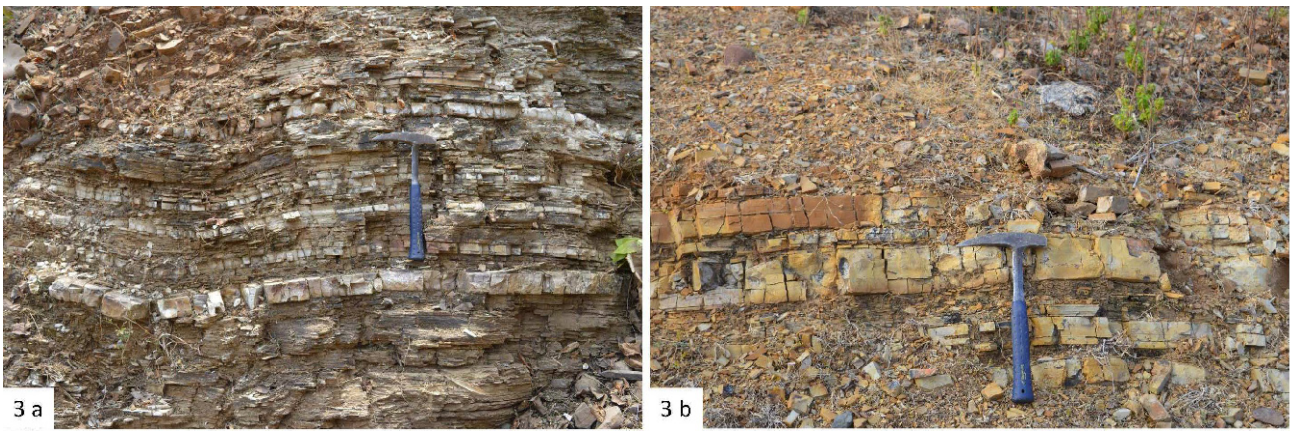

Fig.3. Outcrops of "Lower Kaimur Porcellanite" near **(a)** Badanpur; the blocky ash-grey beds are suspected tuff, and **(b)** Gurserighat; the blocky brownish-weathered ash-grey beds are suspected tuff. The hammer is 35 cm long.

Table 2.. Chemical Composition of the "Lower Kaimur Porcellanite" (Major oxides are reported on LOI-free basis. LOI ranged from 2.63% to 3.77%.)

Unit Symbol	%	%	%	%	%	%	%	%	%	%	ppm	ppm	ppb	ppm	ppm	ppm	ppm	ppm
Detection Limit	0.01	0.01	0.01	0.001	0.01	0.01	0.01	0.01	0.01	0.001	0.01	1	0.1	0.5	0.1	1	1	0.5	0.1
Analysis Method	FUS-ICP	FUS-ICP	FUS-ICP	FUS-ICP	FUS-ICP	FUS-ICP	FUS-ICP	FUS-ICP	FUS-ICP	FUS-ICP	FUS-ICP	FUS-ICP	INAA	INAA	FUS-MS	TD-ICP	FUS-MS	FUS-MS	FUS-MS
Sample	SiO_2	Al_2O_3	Fe_2O_3	MnO	MgO	CaO	Na2O	K_2O	TiO_2	P_2O_5	Ba	Co	Cr	Cs	Cu	Ga	Ge	Hf
JUP1	92.69	5.04	0.68	0.01	0.30	0.13	0.03	0.85	0.18	0.104	353	18.8	13.9	1.7	39	7.0	1.6	1.5
JUP2	91.49	5.64	1.00	0.03	0.35	0.13	0.03	0.96	0.21	0.145	644	12.1	16.9	2.4	48	9.0	1.9	1.9
JUP3	92.19	5.30	0.64	0.04	0.38	0.11	0.03	1.02	0.23	0.052	352	17.4	19.1	2.6	47	8.0	1.7	2.2
JUP4	91.50	5.65	1.04	0.04	0.39	0.11	0.03	0.94	0.23	0.072	373	21.3	16.8	2.7	73	9.0	1.8	2.1
JUP5	90.66	6.71	0.55	0.01	0.37	0.13	0.03	1.04	0.33	0.166	869	12.6	24.6	3.2	19	11.0	2.0	2.4
JUP6	90.22	6.17	1.23	0.01	0.54	0.12	0.02	1.41	0.25	0.031	188	9.1	17.0	3.1	21	10.0	2.2	1.9
JUP7	91.73	5.03	1.34	0.00	0.42	0.09	0.02	1.13	0.17	0.052	184	12.8	15.7	2.4	19	8.0	1.8	1.7
JUP8	86.03	7.65	1.53	0.03	0.37	0.17	0.54	3.36	0.21	0.113	657	21.4	24.8	5.9	30	11.0	1.7	1.7
JUP9	92.81	4.96	0.44	0.00	0.37	0.06	0.02	1.11	0.16	0.062	207	15.0	9.8	3.2	29	6.0	2.0	1.5
JUP10	89.59	6.07	1.66	0.01	0.62	0.18	0.03	1.46	0.19	0.196	345	12.9	19.6	3.6	46	10.0	1.9	1.9
JUP11	89.00	6.23	1.80	0.08	0.53	0.20	0.02	1.54	0.23	0.378	522	45.8	20.6	3.4	40	8.0	1.9	2.0
JUP12	90.93	5.79	0.95	0.02	0.49	0.16	0.02	1.27	0.19	0.188	354	14.5	11.9	2.7	18	8.0	1.9	1.6
JUP13	87.82	7.32	2.02	0.01	0.68	0.20	0.02	1.53	0.21	0.186	327	7.3	17.3	4.1	44	10.0	2.1	2.0
Average	90.51	5.97	1.14	0.02	0.45	0.14	0.07	1.36	0.21	0.13	413	17.0	17.5	3.2	36	8.8	1.9	1.9

Unit Symbol	ppm	ppm	ppm	ppm	%	ppm	ppm	ppm	ppm	ppm	ppm	ppm	ppm	ppm	ppm
Detection Limit	0.2	1	5	1	0.001	0.1	0.01	2	0.01	0.05	0.01	5	1	1	1
Analysis Method	FUS-MS	TD-ICP	TD-ICP	FUS-MS	TD-ICP	INAA	INAA	FUS-ICP	FUS-MS	FUS-MS	FUS-MS	FUS-ICP	INAA	FUS-ICP	MULT INA A /TD-ICP
Sample	Nb	Ni	Pb	Rb	S	Sb	Sc	Sr	Ta	Th	U	V	W	Y	Zn
JUP1	2.3	14		28	0.023	0.4	3.97	41	0.27	4.3	1.3	40	52	18	13
JUP2	2.8	23	11	34	0.006	0.7	5.70	64	0.39	5.4	1.4	45	45	22	41
JUP3	3.1	20	19	36	0.006	0.4	5.76	34	0.37	6.4	2.0	36	34	25	19
JUP4	2.9	37	12	34	0.004	0.5	5.54	37	0.34	5.9	1.5	38	37	22	50
JUP5	4.1	15	69	48	0.004	0.4	7.12	78	0.64	8.4	2.2	69	58	28	37
JUP6	2.9	13	8	49	0.006	0.4	5.92	37	0.30	5.7	1.4	36	25	13	11
JUP7	2.4	11	20	38	0.004	0.3	5.16	56	0.26	4.9	1.1	29	41	13	8
JUP8	3.5	10	15	140	0.005	0.8	6.57	73	0.76	9.0	2.5	70	137	42	36
JUP9	2.4	13		42	0.004	0.2	4.23	23	0.41	4.2	1.0	15	60	12	23
JUP10	2.9	31	54	49	0.009	1.1	5.16	188	0.39	5.0	2.0	87	49	65	162
JUP11	3.0	31	11	52	0.008	0.7	4.99	475	0.34	5.3	2.8	152	98	40	20
JUP12	2.0	13		41	0.004	0.5	4.25	226	0.18	4.4	1.5	51	44	47	15
JUP13	2.6	29	35	52	0.006	0.8	5.87	207	0.32	5.2	2.2	92	20	32	81
Average	2.8	20	25	49	0.007	0.6	5.40	118	0.38	5.7	1.8	58	54	29	40

Unit Symbol	ppm	ppm	ppm	ppm	ppm	ppm	ppm	ppm	ppm	ppm	ppm	ppm	ppm	ppm	ppm	ppm
Detection Limit	1	0.05	0.05	0.01	0.05	0.01	0.005	0.01	0.01	0.01	0.01	0.01	0.05	0.005	0.01	0.002
Analysis Method	FUS-ICP	FUS-MS	FUS-MS	FUS-MS	FUS-MS	FUS-MS	FUS-MS	FUS-MS	FUS-MS	FUS-MS	FUS-MS	FUS-MS	FUS-MS	FUS-MS	FUS-MS	FUS-MS
Sample	Zr	La	Ce	Pr	Nd	Sm	Eu	Gd	Tb	Dy	Ho	Er	Tl	Tm	Yb	Lu
JUP1	56	17.0	32.2	4.7	19.4	4.5	0.89	4.1	0.61	3.37	0.6	1.67	0.17	0.26	1.77	0.291
JUP2	68	16.8	32.3	4.7	18.6	4.0	0.75	3.8	0.6	3.63	0.73	2.18	0.18	0.33	2.31	0.384
JUP3	75	20.3	43.5	5.1	19.4	3.8	0.78	3.5	0.63	4.02	0.88	2.67	0.13	0.41	2.93	0.494
JUP4	78	17.6	36.2	4.5	17.4	3.6	0.69	3.5	0.58	3.69	0.8	2.44	0.07	0.37	2.62	0.422
JUP5	92	46.0	118.0	12.1	42.4	8.0	1.31	6.3	0.96	5.04	0.96	2.94	0.13	0.42	2.89	0.457
JUP6	75	21.0	42.6	5.3	18.9	3.0	0.52	2.3	0.39	2.36	0.47	1.53	0.07	0.24	1.71	0.300
JUP7	62	30.2	47.3	7.3	27.8	5.4	0.94	4.0	0.55	2.85	0.52	1.46		0.22	1.61	0.262
JUP8	68	50.5	71.4	12.2	47.9	9.8	1.82	9.3	1.3	7.29	1.34	3.59	0.47	0.49	3.12	0.472
JUP9	53	12.0	25.5	3.3	12.3	2.4	0.46	2.3	0.38	2.34	0.46	1.3	0.09	0.20	1.34	0.218
JUP10	69	59.3	74.2	16.9	72.2	16.2	3.26	15.5	2.27	12.4	2.21	5.96	0.14	0.82	5.04	0.755
JUP11	70	39.4	56.7	10.9	44.7	10.0	1.98	9.5	1.41	7.72	1.41	3.81	0.21	0.54	3.39	0.526
JUP12	66	31.6	39.7	9.8	43.6	10.7	2.22	11.2	1.68	9.11	1.62	4.31		0.59	3.58	0.552
JUP13	73	93.1	101.0	21.6	79.5	14.5	2.57	10.3	1.31	6.89	1.2	3.13		0.45	3.06	0.463
Average	70	35.0	55.4	9.1	35.7	7.4	1.40	6.6	0.97	5.44	1.02	2.85	0.17	0.41	2.72	0.430

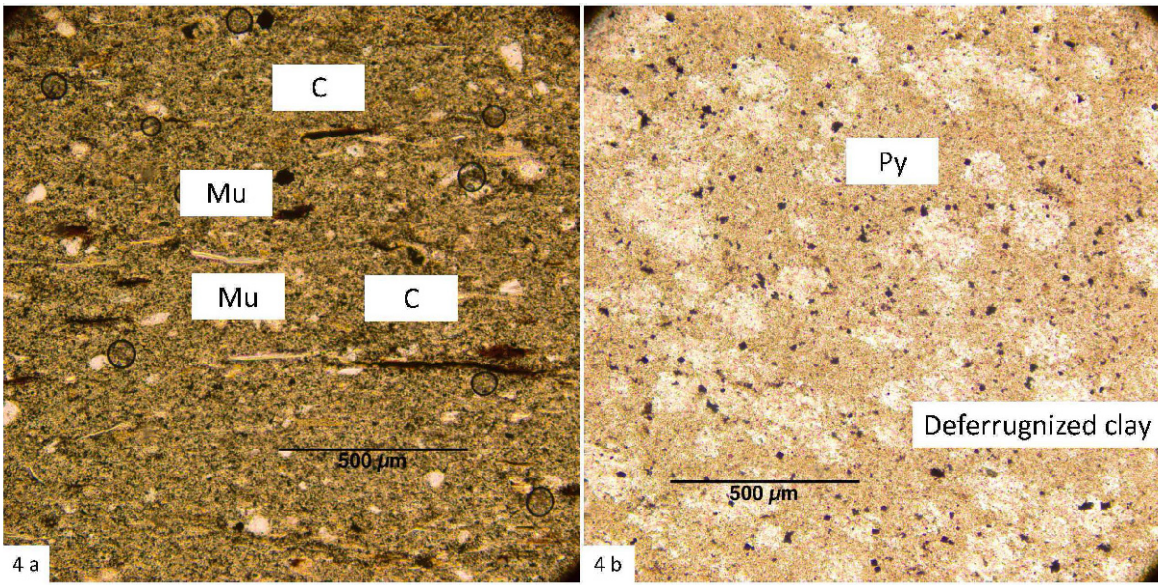

Fig.4. Plane polarized light optical photomicrographs of (a) brown shale with dark elongate carbonaceous particles (C) and muscovite flakes (light elongate; Mu), and (b) light brown shale with deferruginized spots (light); the black grains are pyrite (Py) and carbonaceous specks.

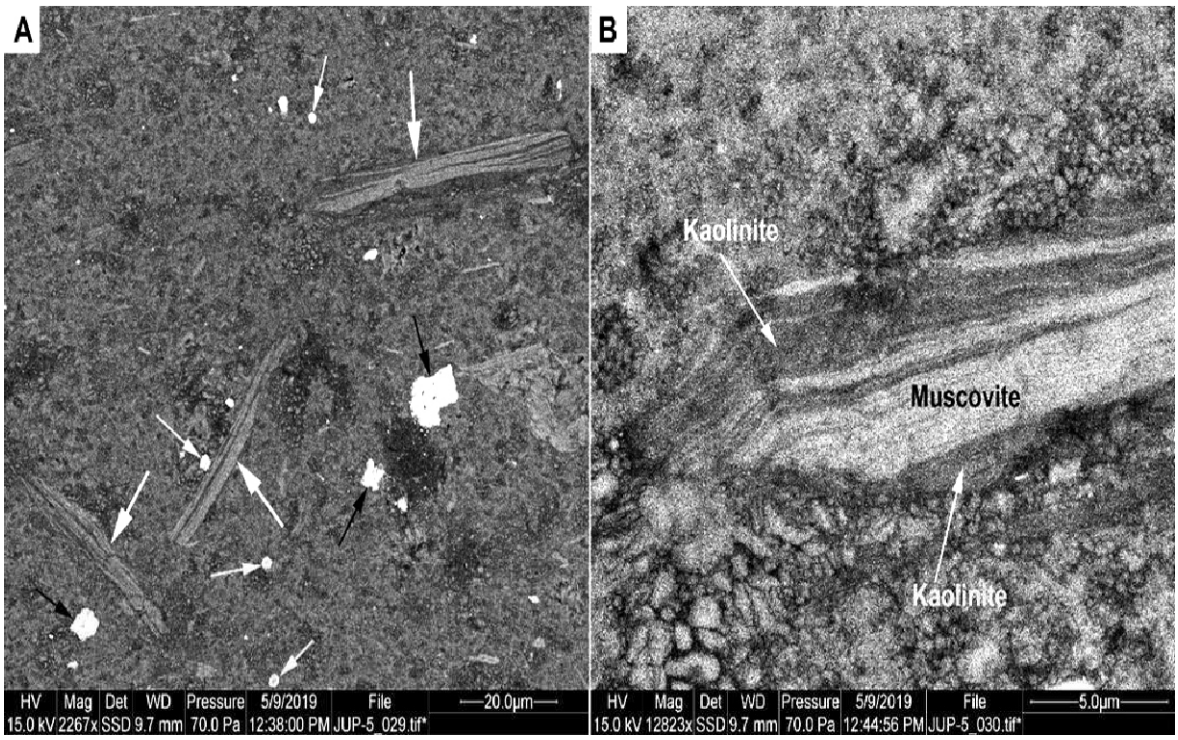

Fig.5. SEM-BSE image of muscovite flakes in fine grained siliceous matrix. **(A)** Muscovite flakes (confirmed by EDS analysis) pointed out by white arrows, black arrows point to Ti-rich particles, and gray arrows point to phosphatic spheres of likely microbial origin (Schieber et al., 2007). **(B)** Detail of muscovite flake. It shows that the striped appearance of muscovite grains in (A) is due to partial alteration of muscovite to kaolinite and consequent "swelling". This diagenetic overprint, as well as deformation, bending and truncation of muscovite layers indicate that the muscovite flakes are of detrital origin. Note scale bars at bottom right.

porcelain" (Bates and Jackson, 1984; p. 397). Silicified shale, mudstone, tuff, limestone, and even some contact metamorphosed sedimentary rocks may qualify to be so named (Teall, 1884). Mallet (1869) described a set of silicified Vindhyan strata in the Son river valley as porcellanite. Auden (1933), with added evidence from optical microscopy, identified these as silicified tuff. The importance of searching for and dating tuff in craton-interior mid-Proterozoic basins cannot be overemphasized. The sedimentary rocks in these basins record global marine anoxia (Derry, 2015; Arnold et al., 2004; Shen et al., 2003), global sulfuric oceans (Lyons et al., 2009; Kah and Bartley, 2011), global Fe-rich oceans (Planavsky et al., 2011), among other attributes that reveal the composition of mid-Protereozoic oceans. Robust dating of magmatic zircons in intercalated tuff beds can document the synchronicity of the sedimentological evolution of these basins and the connectivity of the oceans. Such robust ages could also lead to revised stratigraphy. For example, discovery of K-bentonite beds (tuff) and SHRIMP-dating of zircons therein (~ 1380 Ma) revised the age of the Xiamaling Formation in the North China Craton from Ediacaran to Mesoproterozoic (Su et al., 2008) as is also the case in Chhattisgarh basin in India (Basu et al., 2008).

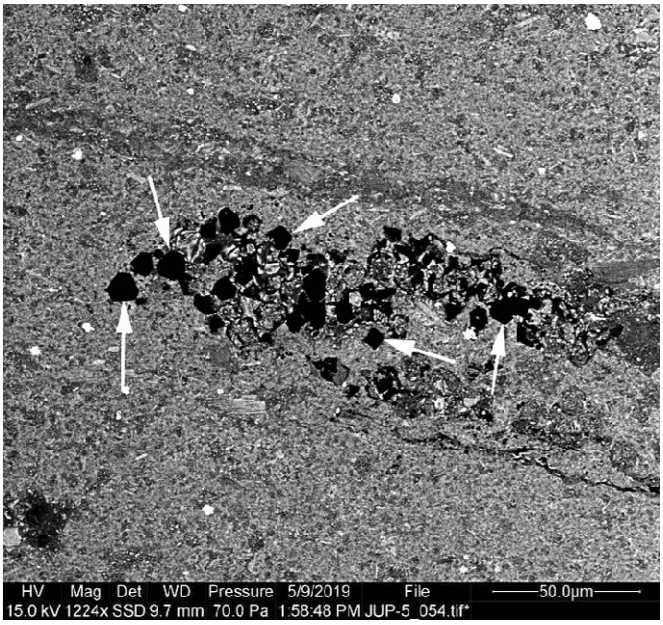

Fig.6. Shape of epoxy-filled cavities (black, pointed out by white arrows) suggests that these are most likely sites of former pyrite crystals that were either plucked out during thin section preparation, or more likely were dissolved in the course of outcrop weathering (SEM-BSE).

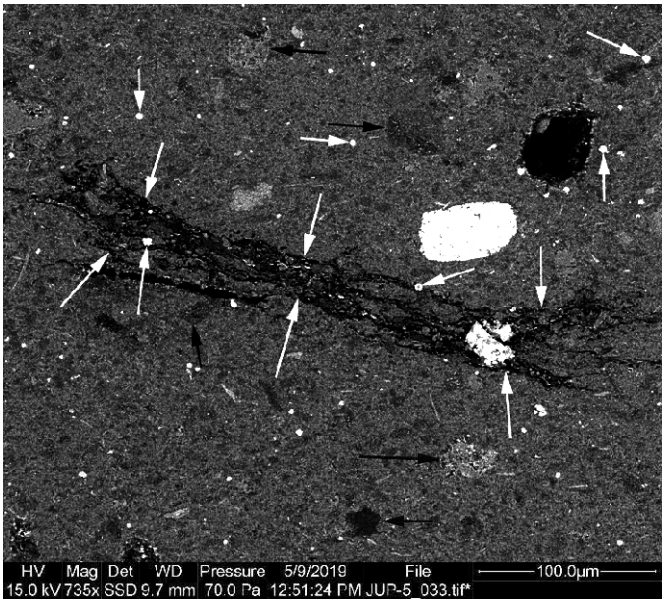

Fig.7. Overview of porcellanite fabric in sample JUP-5 (SEM backscattered image). White arrows point to carbonaceous particle with a wavy-lenticular internal fabric. The fabric resembles eroded microbial mats (Schieber, 1989; Deb et al., 2007). Within the fine grained siliceous groundmass are scattered larger grains (near bottom; black arrows) that appear to be largely mudstone lithics (Schieber and Bennett, 2014; Schieber, 2016; Schieber et al., 2019). The grey arrows point to phosphatic spheres of likely microbial origin (Schieber et al., 2007).

No magmatic activity between approximately 1.6 Ga and 1.1 Ga has been recorded in the Vindhyan Supergroup. This ~ 1.5 billion years of magmatic quiescence is unusual in Earth history. Thorough searches for and identification of tuff especially in the upper Vindhyan (for example, Chakraborti et al., 1996; Sen and Mishra, 2019) are likely to produce encouraging results.

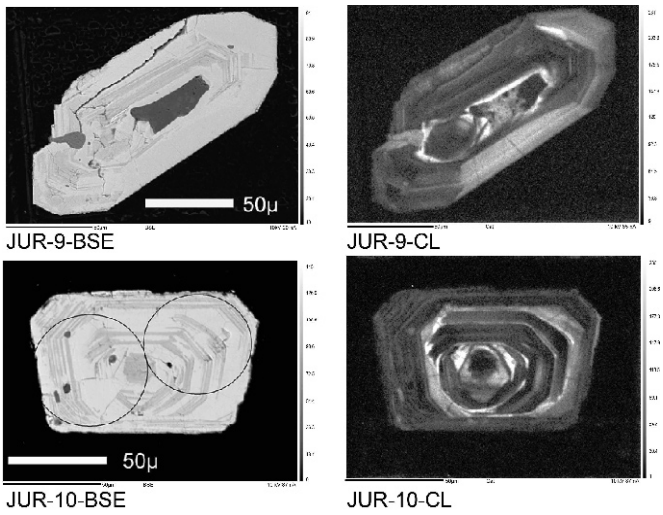

Fig.8. Paired backscattered electron (BSE) and cathodoluminescence (CL) images of magmatically zoned zircon grains (JUR-9; JUR-10).

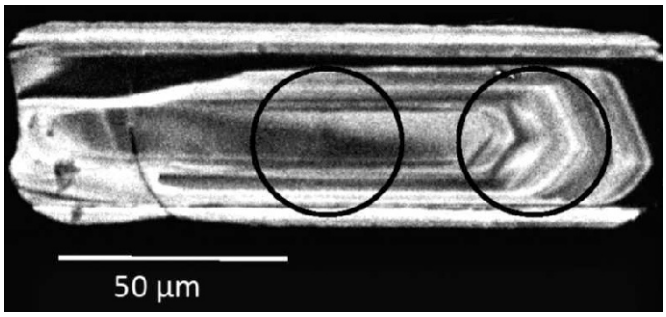

Fig.9. Cathodoluminescence (CL) image of the only magmatically zoned zircon grain (JUR-1) that could be reliably dated.

CONCLUSIONS

Porcellanites are rocks that have the appearance of unglazed porcelain-ware; they are usually silicified mudstones or ash/tuff. Many Proterozoic porcellanites in India are silicified tuffs that are chronostratigraphic marker beds testifying to coeval volcanism. These have immense geological significance, especially in the craton-interior mid-Proterozoic basins in India where chronostratigraphic and biostratigraphic markers are scarce.

A 100 km outcrop extent of a porcellanite bed was thoroughly investigated and informally named “Lower Kaimur Porcellanite”, lying above the lower Kaimur Sandstone (Vindhyan Supergroup) in the western Son river valley. However, it was not possible to find evidence for an igneous origin of this porcellanite bed (LKP). Important facts in this regard are (a) the newly determined U-Pb age of the only analyzable zircon grain in this rock is far older than the studied host formation, and, (b) abundant occurrence of microbial spherules in this rock indicates a sedimentary origin.

Acknowledgements: We gratefully acknowledge the support from Indiana University and Syracuse University. AC was supported by DST INSPIRE Faculty Program, Govt. of India. SS acknowledges the support from DST PURSE II and CAS, Department of Geological Sciences, Jadavpur University. A National Science Foundation equipment grant to J. S. Schieber (EAR-0318769) provided funds for the purchase of the analytical SEM used to acquire the images in this report. Ms. Ruth Droppo kindly adjusted and finalized several illustrations. We thank the extremely helpful anonymous reviewer and the editor at whose advice we have removed extraneous matter and improved the text.

References

Arnold, G.L., Anbar, A.D., Barling, J., and Lyons, T.W. (2004) Molybdenum isotope evidence for widespread anoxia in mid-Proterozoic oceans. Science, v.304, pp.87-90.

Auden, J.B. (1933) Vindhyan sedimentation in the Son Valley, Mirzapur District. Mem. Geol. Surv. India, v.62, pp.141-250.

Basu, A., Patranabis-Deb, S., Schieber, J., and Dhang, P. (2008) Stratigraphic position of the ~1000 Ma Sukhda Tuff (Chhattisgarh Supergroup, India) and the 500 Ma question. Precambrian Res., v.167, pp.383-388.

Basu, A., Bickford, M.E., and Deasy, R. (2016) Inferring tectonic provenance of siliciclastic rocks from their chemical compositions: A dissent. Sedimentary Geology, v.336, pp.26-35.

Bates, R. L. and Jackson, J. A. (1984) Dictionary of Geological Terms. Geological Institute (Anchor Books). 571 p.

Bellot, N., Boyet, M., Doucelance, R., Bonnand, P., Savov, I.P., Plank, T., and Elliott, T. (2018) Origin of negative cerium anomalies in subduction-related volcanic samples: Constraints from Ce and Nd isotopes. Chemical Geol., v.500, pp.46-63.

Bhattacharyya, A. and Morad, S. (1993) Proterozoic braided ephemeral fluvial deposits: an example from the Dhandraul Sandstone Formation of the Kaimur Group, Son Valley, central India. Sedimentary Geol., v.84, pp.101-114.

Bickford, M.E., Basu, A., Patranabis-Deb, S., Dhang, P.C., and Schieber, J. (2011a) Depositional history of the Chhattisgarh basin, central India: Constraints from new SHRIMP zircon ages. Jour. Geol., v.119, pp.33-50.

Bickford, M.E., Basu, A., Mukherjee, A., Hietpas, J., Schieber, J., Patranabis-Deb, S., Ray, R.K., Guhey, R., Bhattacharya, P., and Dhang, P.C. (2011b) New U-Pb SHRIMP zircon ages of the Dhamda Tuff in the Mesoproterozoic Chhattisgarh basin, Peninsular India: Stratigraphic implications and significance of a 1-Ga thermal-magmatic event. Jour. Geol., v.119, pp.535-548.

Bickford, M.E., Saha, D., Schieber, J., Kamenov, G., Russell, A., and Basu, A. (2013) New U-Pb ages of zircons in the Owk Shale (Kurnool Group) with reflections on Proterozoic porcellanites in India. Jour. Geol. Soc. India, v.82, pp.207-216.

Bickford, M.E., Basu, A., Kamenov, G.D., Mueller, P.A., Patranabis-Deb, S., and Mukherjee, A. (2014) Petrogenesis of 1000 Ma felsic tuffs, Chhattisgarh and Indravati basins, Bastar craton, India: Geochemical and Hf isotope constraints. Jour. Geol., v.122, pp.43-54.

Bickford, M.E., Mishra, M., Mueller, P.A., Kamenov, G.D., Schieber, J., and Basu, A. (2017) U-Pb age and Hf isotopic compositions of magmatic zircons from a rhyolite flow in the Porcellanite Formation in the Vindhyan Supergroup, Son Valley (India): implications for its tectonic significance. Jour. Geol., v.125, pp.367-379.

Bora, S., Kumar, S., Yi, K., Kim, N., and Lee, T.H. (2013) Geochemistry and U-Pb SHRIMP zircon chronology of granitoids and microgranular enclaves from Jhirgadandi Pluton of Mahakoshal Belt, Central Indian Tectonic Zone, India. Jour. Asian Earth Sci., v.70-71, pp.99-114.

Bose, P.K., Sarkar, S., Chakrabarty, S., and Banerjee, S. (2001) Overview of the Meso- to Neoproterozoic evolution of the Vindhyan basin, central India. Sedimentary Geol., v.141-142, pp.395-419.

Calcera, P. (1847) Esposizione Metodica Delle Rocce E dei Terreni del Globo Coll'indicazione Dei Principali Esempii della Sicilia. Pagano, Palermo. 32 p.

Chakraborti, S. (1997) Elucidation of the sedimentary history of the Singhora Group of rocks, Chhattisgarh Supergroup, M.P. Rec. Geol. Surv. India, v.130, pp.180-187.

Chakraborty, C. (2006) Proterozoic intracontinental basin: the Vindhyan example. Jour. Earth System Sci., v.115, pp.3-22.

Chakraborty, C. and Bose, P.K. (1990) Internal structures of sandwaves in a tide-storm interactive system: Proterozoic Lower Quartzite Formation, India. Sedimentary Geol., v.67, pp.133-142.

Chakraborty, P.P. (2006) Outcrop signatures of relative sea level fall on a siliciclastic shelf: Examples from the Rewa Group of Proterozoic Vindhyan Basin. Jour. Earth System Sci., v.115, pp.23-36.

Chakraborty, P.P., Banerjee, S., Das, N.G., Sarkar, S., and Bose, P.K. (1996) Volcaniclastics and their sedimentological bearing in Proterozoic Kaimur and Rewa groups in central India. Mem. Geol. Soc. India, v.36, pp.59-75.

Das, K., Yokoyama, K., Chakraborty, P.P., and Sarkar, A. (2009) Basal tuffs and contemporaneity of the Chattisgarh and Khariar Basins based on new dates and geochemistry. Jour. Geol., v.117, pp.88-102.

Das, K., Chakraborty, P.P., Hayasaka, Y., Kayama, M., Saha, S., and Kimura, K. (2015) *c.* 1450 Ma regional felsic volcanism at the fringe of the East Indian Craton: constraints from geochronology and geochemistry of tuff beds from detached sedimentary basins. Geol. Soc., London, Mem., v.43, pp.207-221.

Deb, S. P., Schieber, J., and Chaudhuri, A. K. (2007) Microbial mat features in mudstones of the Mesoproterozoic Somanpalli Group, Pranhita-Godavari Basin, India. *In:* Schieber, J., Bose, P. K., Eriksson, P. G., Banerjee, S., Sarkar, S., Alterman, W., and Catunneanu, O. (Eds.) Atlas of Microbial Mat Features Preserved within the Siliciclastic Rock Record. pp.171-180.

Denduluri, D.V.S., Mukherjee, A., Balaram, V., and Nagaraju, K. (2006) Proterozoic felsic volcanism in the Chhattisgarh Sedimentary basin, Central India: Its implications on the basin evolution (Abstract). Asia-Oceania Geosciences Society 3rd Annual Meeting.

Derry, L.A. (2015) Causes and consequences of mid-Proterozoic anoxia. Geophys. Res. Lett., v.42, pp.8538-8546.

Ghosh, S.K. (1971) Petrology of the porcellanite rocks of Samaria area, Sidhi Dist., M.P. Quart. Jour. Geol., Min. Metall. Soc. India, v.43, pp.153-164.

Gupta, S., Jain, K.C., Srivastava, V.C., and Mehrotra, R.D. (2003) Depositional environment and tectonism during the sedimentation of the Semri and Kaimur Groups of rocks, Vindhyan Basin. Jour. Palaeontol. Soc. India, v.48, pp.181-190.

Holland, H.D. (2006) The oxygenation of the atmosphere and oceans. Phil. Trans. Royal Soc. B: Biological Sciences, v.361, pp.903-915.

Kah, L.C. and Bartley, J.K. (2011) Protracted oxygenation of the Proterozoic biosphere. Internat. Geol. Rev., v.53, pp.1424-1442.

Kale, V.S. (2016) Proterozoic basins of Peninsular India: status within the global Proterozoic systems. Proc. Indian National Sci. Acad., v.82, pp.461-477.

Lyons, T.W., Anbar, A.D., Severmann, S., Scott, C., and Gill, B.C. (2009) Tracking euxinia in the ancient ocean: a multiproxy perspective and Proterozoic case study. Annual Rev. Earth Planet. Sci., v.37, pp.507-534.

Mallet, F.R. (1869) On the Vindhyan Series, as exhibited in the north-western and central Provinces of India. Mem. Geol. Surv. India, v.7, pp.1-129.

Mandal, S., Choudhuri, A., Mondal, I., Sarkar, S., Chakraborty, P.P., and Banerjee, S. (2019) Revisiting the boundary between the Lower and Upper Vindhyan, Son valley, India. Jour Earth Systems Sci, v.128, 222. DOI:10.1007/s12040-019-1250-2

Mishra, M., Bickford, M.E., and Basu, A. (2018) U-Pb Age and Chemical Composition of an ash bed in the Chopan Porcellanite Formation, Vindhyan Supergroup, India. Jour. Geol., v.126, pp.553-560.

Mishra, M., Srivastava, V., Sinha, P.K., and Srivastava, H.B. (2017) Geochemistry of Mesoproterozoic Deonar pyroclastics from Vindhyan Supergroup of central India: Evidences of felsic magmatism in the Son Valley. Jour. Geol. Soc. India, v.89, pp.375-385.

Mukherjee, A., Bickford, M.E., Hietpas, J. , Schieber, J., and Basu, A. (2012) Implications of a newly dated ca. 1000 Ma rhyolitic tuff in the Indravati basin, Bastar craton, India. Jour. Geol., v.120, pp.477-485.

Patranabis-Deb, S., Bickford, M.E., Hill, B., Chaudhuri, A.K., and Basu, A. (2007) SHRIMP ages of zircon in the uppermost tuff in Chattisgarh Basin in central India require ~500 Ma adjustment in Indian Proterozoic stratigraphy. Jour. Geol., v.115, pp.407-415.

Planavsky, N.J., McGoldrick, P., Scott, C.T., Li, C., Reinhard, C.T., Kelly, A.E., Chu, X., Bekker, A., Love, G.D., and Lyons, T.W. (2011) Widespread iron-rich conditions in the mid-Proterozoic ocean. Nature, v.477, pp.448-451.

Quasim, M.A., Khan, I., and Ahmad, A.H.M. (2017) Integrated petrographic, mineralogical, and geochemical study of the upper Kaimur Group of rocks, Son Valley, India: Implications for provenance, source area weathering and tectonic setting. Jour. Geol. Soc. India, v.90, pp.467-484.

Quasim, M.A. and Ahmad, A.H.M. (2015) Petrofacies and tectonic setup of Kaimur Group of rocks, Son Valley, India. The Palaeobotanist, v.64, pp.1-11.

Radhakrishna, B. P. (1987) Purãna Basins of Peninsular India. Mem. Geol. Soc. India, no.6, 518p.

Ramakrishnan, M. and Vaidyanadhan, R. (2010) Geology of India. Geological Society of India, Bangalore, v.1, 552 p.

Rasmussen, B., Bose, P.K., Sarkar, S., Banerjee, S., Fletcher, I.R., and McNaughton, N.J. (2002) 1.6 Ga U-Pb zircon age for the Chorhat Sandstone, Lower Vindhyan, India: Possible implications for early

evolution of animals. Geology, v.30, pp.103-106.

Ray, J.S., Martin, M.W., Veizer, J., and Bowring, S.A. (2002) U-Pb zircon dating and Sr isotope systematics of the Vindhyan Supergroup, India. Geology, v.30, pp.131-134.

Rogers, J.J.W. (1996) A history of continents in the past three billion years. Jour. Geol., v.104, pp.91-107.

Saha, D. and Tripathy, V. (2012) Tuff beds in Kurnool subbasin, southern India and implications for felsic volcanism in Proterozoic intracratonic basins. Geoscience Frontiers, v.3, pp.429-444.

Sarkar, S., Banerjee, S., Chakraborty, S., and Bose, P.K. (2002a) Shelf storm flow dynamics: insight from the Mesoproterozoic Rampur Shale, central India. Sedimentary Geol., v.147, pp.89-104.

Sarkar, S., Chakraborty, S., Banerjee, S., and Bose, P. K. (2002b) Facies sequence and cryptic imprint of sag tectonics in late Proterozoic Sirbu Shale, central India. *In:* Alterman, W. and Corcoran, P. L. (Eds.) Precambrian Sedimentary Environments: A Modern Approach to Ancient Depositional Systems. Internat. Assoc. Sedimentol. Spec. Publ., no.33, pp. 339-350.

Sarkar, S., Eriksson, P.G., and Chakraborty, S. (2004) Epeiric sea formation on Neoproterozoic supercontinent break-up: A distinctive signature in coastal storm bed amalgamation. Gondwana Res., v.7, pp.313-322.

Sarkar, S., Banerjee, S., Eriksson, P.G., and Catuneanu, O. (2005) Microbial mat control on siliciclastic Precambrian sequence stratigraphic architecture. Sedimentary Geol., v.176, pp.195-209.

Schieber, J. (1989) Pyrite mineralization in microbial mats from the mid-Proterozoic Newland Formation, Belt Supergroup, Montana, U.S.A. Sedimentary Geol., v.64, pp.79-90.

Schieber, J. (2016) Mud re-distribution in epicontinental basins: Exploring likely processes. Marine Petrol. Geol., v.71, pp.119-133.

Schieber, J. and Bennett, R. (2013) Bedload transport of mud across a wide, storm-influenced ramp: Cenomanian-Turonian Kaskapau Formation, western Canada foreland basin: Discussion. Jour. Sediment. Res., v.83, pp.1198-1199.

Schieber, J., Sur, S., and Banerjee, S. (2007) Benthic microbial mats in black shale units from the Vindhyan Supergroup, Middle Proterozoic of India: the challenges of recognizing the genuine article. *In:* Schieber, J., Bose, P. K., Eriksson, P. G., Banerjee, S., Sarkar, S., Alterman, W., and Catunneanu, O. (Eds.) Atlas of Microbial Mat Features Preserved within the Siliciclastic Rock Record. pp. 189-197.

Schieber, J., Miclăuº, C., Seserman, A., Liu, B., and Teng, J. (2019) When a mudstone was actually a "sand": results of a sedimentological investigation of the bituminous marl formation (Oligocene), eastern Carpathians of Romania. Sedimentary Geol., v.384, pp.12-28.

Sen, S., Mishra, M., and Patranabis-Deb, S. (2014) Petrological study of the Kaimur Group sediments, Vindhyan Supergroup, Central India: implications for provenance and tectonics. Geosci. Jour., v.18, pp.307-324.

Sen, S. and Mishra, M. (2019) Significance of the tuffaceous beds associated with the Bijaigarh Shale of the Kaimur Group, Vindhyan Supergroup, Central India and their correlation with tuffs in other contemporaneous Proterozoic basins. Jour. Earth System Sci., v.128, : 217. DOI: 10.1007/s12040-019-1212-8

Shen, Y., Knoll, A.H., and Walter, M.R. (2003) Evidence for low sulphate and anoxia in a mid-Proterozoic marine basin. Nature, v.423, pp.632-635.

Shields, G.A. and Stille, P. (2001) Diagenetic constraints on the use of cerium anomalies as palaeoseawater redox proxies: an isotopic and REE study of Cambrian phosphorites. Chemical Geol., v.175, pp.29-48.

Su, W., Zhang, S., Huff, W.D., Li, H., Ettensohn, F.R., Chen, X., Yang, H., Han, Y., Song, B., and Santosh, M. (2008) SHRIMP U-Pb ages of K-bentonite beds in the Xiamaling Formation: Implications for revised subdivision of the Meso- to Neoproterozoic history of the North China Craton. Gondwana Res., v.14, pp.543-553.

Teall, J.J.H. (1884) On the chemical and microscopical characters of the Whin Sill. Quart. Jour. Geol. Soc. London, v.40, pp.640-657.

Tripathy, G.R. and Singh, S.K. (2015) Re-Os depositional age for black shales from the Kaimur Group, Upper Vindhyan, India. Chemical Geol., v.413, pp.63-72.

(Received: 31 May 2019; Revised form accepted: 10 October 2019)